FULL PAPER

Preparation of Engineered *Salmonella Typhimurium*-Driven Hyaluronic-Acid-Based Microbeads with Both Chemotactic and Biological Targeting Towards Breast Cancer Cells for Enhanced Anticancer Therapy

Saji Uthaman, Shaohui Zheng, Jiwon Han, Young Jin Choi, Sunghoon Cho, Van Du Nguyen, Jong-Oh Park, Seung-Hwan Park, Jung-Joon Min, Sukho Park, and In-Kyu Park**

In this study, a new type of targeted bacteriobots is prepared and investigated as a therapeutic strategy against solid tumors. Maleimide-functionalized hyaluronic acid (HA) polymer is synthesized and cross-linked with four-arm-thiolated polyethylene glycol (PEG-SH) to form HA microbeads with diameter of 8 μm through the Michael-type addition. Docetaxel (DTX)-loaded nanoparticles are encapsulated in HA–PEG microbeads and sustained in vitro drug-release pattern of the DTX from the HA–PEG microbeads is observed for up to 96 h. Dual-targeted bacteriobots are prepared using CD 44 receptor-targeted HA microbeads synthesized via microfluidics, followed by the attachment of the flagellar bacterium *Salmonella typhimurium*, which have been genetically engineered for tumor targeting, onto the surface of the HA microbeads by the specific interaction between streptavidin on the HA beads and biotin on the bacteria. After the attachment of bacteria, the bacteriobots show an average velocity of 0.72 μm s^{-1} and high chemotactic migration velocity of 0.43 μm s^{-1} towards 4T1 cells lysates. CD 44 receptor-specific cellular uptake is verified through flow cytometry analysis and confocal imaging, demonstrating enhanced intracellular uptake in CD 44 receptor positive tumor cells compared to normal cells. Therefore, the present study suggests that these bacteriobots have dual-tumor-targeting abilities displaying their potential for targeted anticancer therapy.

1. Introduction

Cancer is a major public health concern and the second leading cause of death across the world. It is projected that a total of 1 658 370 new cancer cases and 589 430 cancer deaths will occur in the United States in 2015.[1] Among currently available therapeutic options, chemotherapy remains a frontline option for the treatment of cancer. However, major drawbacks of chemotherapy are the severe side effects and toxicity issues arising due to the systematic accumulation of the chemotherapeutic drug.[2] In addition, the efficacy of the chemotherapy may decrease over time due to the development of multidrug resistance (MDR) by tumor cells.[3] In order to address these obstacles, an attractive approach is the use of a carrier system that can selectively deliver a cytotoxic dose of drug to cancer cells. This type of tumor-targeting delivery system usually comprises a tumor-targeting natural or synthetic polymer encapsulating a chemotherapy drug. This type of delivery system can control the release of the drug at the tumor site and minimize the side effects to other organs.

Hyaluronic acid (HA) is a naturally occurring biodegradable, biocompatible, and nonimmunogenic linear polysaccharide consisting of alternating disaccharide units of D-glucuronic acid and D-*N*-acetyl-glucosamine linked by alternate β (1→4) interglyosidic linkages.[4] It is also an essential constituent of the extracellular matrix (ECM) and synovial fluid, and more than 50% of the HA in the body is present in the skin, lung, intestines, and ECM. The homeostasis of HA in the body is regulated by the degradation of HA by HA-specific receptors in the lymphatic system, blood, and kidneys.[5,6] There are many types of HA receptors, such as cluster determinant 44 (CD 44),[7] receptor for hyaluronate-mediated motility (RHAMM),[8] HA receptor for endocytosis (HARE)[9] and lymphatic vessel endothelial hyaluronan receptor-1 (LYVE-1).[6,10] Among these,

S. Uthaman, Prof. I.-K. Park
Department of Biomedical Science and BK21 PLUS Center for Creative Biomedical Scientists
Chonnam National University Medical School
160 Baekseo-ro, Gwangju 501-746, Republic of Korea
E-mail: pik96@chonnam.ac.kr
S. Zheng, Dr. J. Han, Y. J. Choi, S. Cho, V. D. Nguyen, Prof. J.-O. Park, Prof. S. Park
School of Mechanical Engineering
Chonnam National University
77 Yongbong-ro, Gwangju 500-757, Republic of Korea
E-mail: spark@jnu.ac.kr
Dr. S.-H. Park, Prof. J.-J. Min
Department of Nuclear Medicine
Chonnam National University Medical School
Gwangju 501-746, Republic of Korea

DOI: 10.1002/adhm.201500556

the principal receptor for HA is CD 44.[11] Furthermore, CD 44 is a target receptor for cancer therapy due to the overexpression of CD 44 receptors on cancer cells.[12] Another unique characteristic of the HA-based systems is the rapid degradation of HA in the cytosol of the tumor cells by hyaluronidases, which are abundant in cytoplasmic compartments, thereby enabling the temporal release of the inner cargo in tumor cells.[13]

Among the different types of drug delivery systems (DDS) currently present, the use of microspheres or microbeads as DDS has many advantages including augmented effectiveness and reduced toxicity of the incorporated anticancer drug to non-targeted cells or tissues. Apart from these, the microbeads could also act a depot of drug near to the tumor cells. The success of these microbeads-based DDS systems depends on the size of the microbeads and mode of administration (intravenous or intra-arterial).[14] Metastatic tumor usually gets their blood supply from the arterial circulation rather than the portal circulation. For example 30 μm (diameter) microbeads containing yttrium-90 are injected through hepatic catheter to arterial supply of tumor.[15] In case of metastatic breast cancer, drugs are usually delivered through catheter, which is surgically implanted directly into the subclavian artery or into a branch of subclavian artery usually thyrocervical trunk. A more selective perfusion could be accomplished by the direct angiographic placement of the catherers into the internal mammary arteries. When administrated intra-arterially these microbeads would be carried by the blood flow to the capillary bed where they would be embolize and release the drug to the target cells or tissue.

Our research group has investigated bacterial-driven microbeads (bacteriobots) for tumor targeting.[16] After the attachment of the attenuated flagellar bacterium *Salmonella Typhimurium* (*S. Typhimurium*), bacteriobots exhibited higher migration velocity towards tumor cell lysate than towards normal cell lysate. Furthermore, these bacteria can also target and accumulate specifically in cancer tissue by recognizing the chemosignals secreted from cancer cells through chemoreceptors on cell membranes in vivo.[17] Due to these characteristics of *S. typhimurium,* it is considered a promising candidate for the development of tumor-targeting bacteria-based microrobots. Several groups have developed various bacteria-actuated microrobots with different particles and bacteria strains, such as polystyrene (PS) beads,[16] polyethylene glycol (PEG)[18] and alginate beads,[19] and liposomes.[20] However, these studies have only demonstrated the ability of the bacteria-driven microrobots to migrate towards tumor cells or cell lysate. Enhanced therapeutic efficacy mediated by tumor-targeting bacteria and their ability to carry anticancer drugs remains to be demonstrated. A variety micro-/nanorotors comprising of artificial bacterial flagella (ABF) similar in properties to that of natural bacterial flagella have been developed, which are capable of accomplishing precise 3D swimming in liquids.[21] However, the ABF were only actuated and steered upon a continuous supply of rotating magnetic field, as they do not have an on-board power source. Apart from these, the artificial flagella developed also lacks self-targeting capabilities towards tumor cells. There have been attempts made to develop microbiorobots in which a single motile cell (sperm cell) is trapped inside the tube cavity of the microtube.[22] Microtubes were fabricated by rolling up thin sheets of ferromagnetic layers, which helps in the separation of selected sperm driven microbiorobots and also in controlling the direction of microbiorobot movement. Ferrite-coated cytocompatible nanopropellers have been also developed,[23] which can be maneuvered in a rotating magnetic field. Interestingly till date all the ABF-based systems use magnetic-based head or coating for their propelling action. In nature, biological motors like bacterial flagellum directly converts chemical free energy to mechanical power by generating isothermal and non-equilibrium state through various biochemical reactions such as metabolism of chemicals by cells to synthesis products, which could be used as energy resources. For example, the use of transmembrane receptors of the bacteria to bind targets and controls their directional movement by sensing the chemical gradient. Chemotaxis motion is the movement of cell or organism up or down a chemical gradient in response to an attractant or repellant. Metastatic cancer cells also used migration to move out from primary tumor and colonize in other organs.[24] Even though many ABF-based systems have been developed, which has the self-propelling property similar to that of the bacterial flagella, however till date there is no report for an ABF that could target the cells based on chemotaxis or has chemotaxis-based movement.

Here, we hypothesized that a dual-targeted bacteriobot system could be developed for both tumor targeting and anti-tumor therapy by producing microbeads incorporated with anticancer drugs with maleimide-modified CD 44-specific HA and PEG-SH, followed by attaching attenuated *S. typhimurium* in a spatially controlled manner to allow motility toward the tumor cells. To our knowledge, there is no comprehensive study involving a dual-targeted bacteria-driven microbead-based drug delivery system (DDS) that targets both CD 44 and chemokine receptors. In our study, HA polymer was used to synthesize the microbeads due to its specific tumor cell targeting via CD 44 receptors. The tumor-targeting attenuated *S. typhimurium* was attached to the surface of HA microbeads via streptavidin–biotin conjugation, facilitating CD 44 receptor and bacterial chemo-receptor-mediated tumor targeting. For the incorporation of both chemical and biological anticancer effects in dual-tumor-targeting bacteria-driven microbeads, docetaxel (DTX), an anti-mitotic chemotherapy drug, was encapsulated in poly(lactide-*co*-glycolide) (PLGA). The PLGA–DTX nanoparticles were subsequently embedded inside the microbeads prior to bacterial attachment. The physiochemical characterizations, in vitro cytotoxicity, and cellular uptake of the dual targeted bacteria-driven microbeads were investigated in this study.

2. Results and Discussion

2.1. Synthesis and Characteristics of Drug Nanoparticle-Encapsulated HA Microbeads

2.1.1. Synthesis of Maleimide-Functionalized HA

Maleimide-functionalized HA polymer (HA-Mal) was prepared by reacting HA and *N*-(2-aminoethyl) maleimide trifluoroacetate salt (AEM) through 1-ethyl-3-(3-dimethylaminopropyl)-carbodiimide (EDC)/*N*-hydroxysuccinimide (NHS) reaction

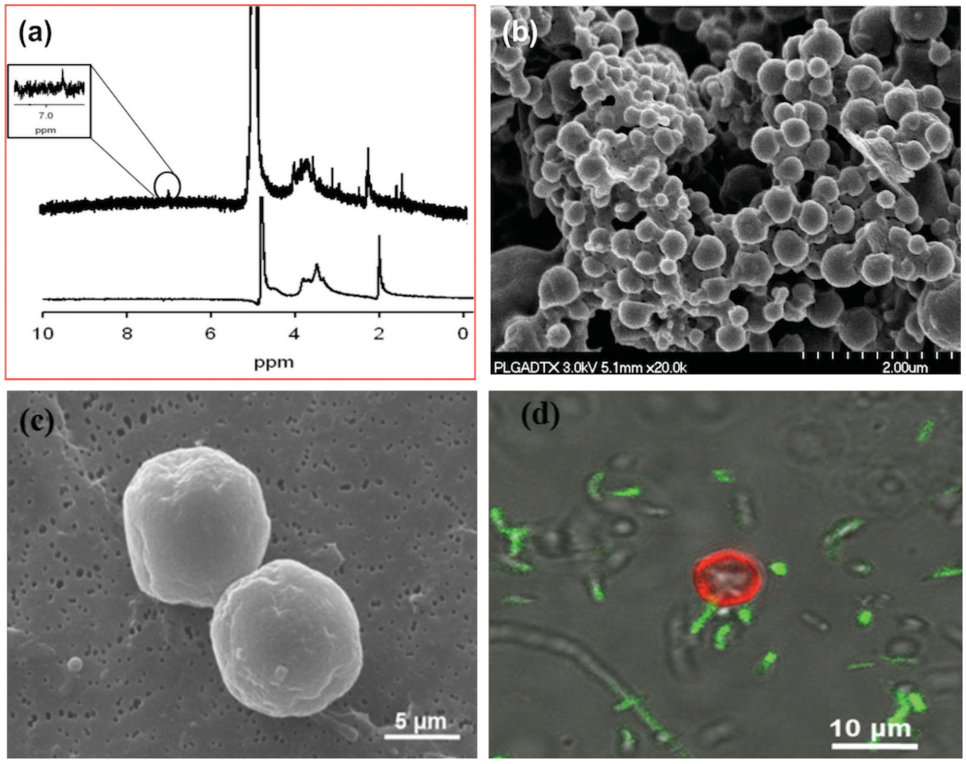

Figure 1. a) ^{1}H NMR spectra of HA and HA-Mal (D_2O). b) Scanning electron microscope image of PLGA–DTX nanoparticles. c) Scanning electron microscope image of HA–PEG microbeads. d) Confocal microscopic image of HA microbeads attached to the bacteria (bacteriobot).

(Figure S1, Supporting Information**)**. The reaction was performed in 0.1 M 2-(N-morpholino)ethane sulfonic acid (MES) buffer for 4 h. The resulting HA-Mal polymer was purified using dialysis and freeze-dried. ^{1}H NMR analysis was performed to determine the degree of substitution (DS) of the HA-Mal, which is defined as the number of maleimide groups per 100 disaccharide rings of HA. The ^{1}H NMR spectrum (**Figure 1**a) of the synthesized HA-Mal showed signal at δ 6.8 corresponding to the vinyl protons of the maleimide and at δ 2.0 for the acetylamine methyl protons of HA.[25] The DS (%) of maleimide in HA-Mal was determined from the ^{1}H NMR spectrum by peak integration of the *N*-acetyl group of HA and the vinyl group of maleimide at δ 2.0 and δ 6.8, respectively, and found to be 20%.

2.1.2. Preparation of PLGA–DTX Nanoparticles

PLGA–DTX nanoparticles were prepared using the solvent evaporation method, and the average hydrodynamic diameter and zeta potential of the nanoparticles were determined using dynamic light scattering (DLS). The average hydrodynamic diameter of the PLGA–DTX nanoparticles was 277 ± 5.38 nm, and the zeta potential value was −1.58 ± 5.28 mV (Figure S2, Supporting Information). The morphology of the nanoparticles was analyzed via scanning electron microscope (SEM) analysis and found to be spherical (Figure 1b). The DTX encapsulation efficiency was 87.5%, as determined by high-performance liquid chromatography (HPLC) analysis. It has been previously reported that the size of the nanoparticles plays a major role in their efficacy because they must easily infiltrate the tumor cell with an average pore size of 400 nm.[26] Therefore, upon release from the microbeads, the synthesized PLGA–DTX nanoparticles could easily penetrate inside the tumor.

2.1.3. Preparation of Nanoparticle-Loaded HA Microbeads

HA microbeads were prepared via the Michael-type addition cross-linking between the maleimide-functionalized HA and PEG–SH. HA microbeads were synthesized by cross-linking the PEG–SH droplet with an aqueous solution of HA-Mal, washed, lyophilized, and observed by SEM. As shown in Figure 1c, the HA–PEG microbeads had a uniformly spherical shape and rough surface with an average diameter about 8 μm. The zeta potential of the HA microbeads was determined as −8.71 ± 2.46 mV. In PBS, no significance degradation was noticed till 48 h and the structural integrity is also maintained. The diameter of microbeads could be adjusted by regulating the flow rate ratio between the continuous phase (CP) and dispersed phase (DP). Due to the hydrophilic nature of the HA-Mal and PEG–SH, it is extremely hard to entrap the hydrophobic DTX; hence, DTX was encapsulated in PLGA and mixed with PEG–SH. The resultant droplets were cross-linked with HA-Mal to form the nanoparticle-loaded microbeads. The encapsulation efficiency of the PLGA–DTX nanoparticles in the HA microbeads was found to be 75%.

2.1.4. In Vitro Release Profile of DTX from PLGA–DTX Nanoparticle-Loaded Microbeads

The in vitro drug release of the PLGA–DTX nanoparticles and HA microbeads was investigated using the dialysis bag method in phosphate-buffered saline (PBS) (pH 7.4) at 37 °C and measured by HPLC. As shown in Figure S3 (Supporting Information), the PLGA–DTX nanoparticles rapidly released approximately 75% and 95% of the encapsulated DTX in 24 h and 96 h, respectively. However, the PLGA–DTX nanoparticle-encapsulated HA–PEG microbeads released only approximately 38% and 65% of DTX in 24 h and 96 h, respectively. The results demonstrated that DTX release was delayed by encapsulating PLGA–DTX nanoparticles in the HA–PEG microbeads synthesized through a cross-junction microchannel with a diameter of approximately 8 µm. The drug was released in a moderate and continuous manner. The entrapment of the PLGA–DTX nanoparticles in the HA microbeads delayed the release of DTX and continuously supplied drug to the surrounding medium so that the microbeads maintained a steady therapeutic effect. These results demonstrate that HA microbeads can act as an excellent drug reservoir platform.

2.1.5. In Vitro Cell Cytotoxicity of PLGA–DTX Nanoparticle-Loaded Microbeads

Cell viability following treatment with the PLGA–DTX nanoparticle-loaded microbeads was investigated using NIH/3T3 and 4T1 cells for 24 h. As shown in Figure S4a (Supporting Information), the NIH/3T3 cells maintained high cell viability of 80%. However, the 4T1 cells were sensitive to the concentration of DTX with an LD_{50} of 123.7×10^{-9} M.

2.2. Synthesis and Characteristics of Dual-Tumor-Targeting Bacteriobots

2.2.1. Preparation of Dual-Tumor-Targeting Bacteriobots by Immobilizing S. Typhimurium on PLGA–DTX Nanoparticle-Encapsulated HA Microbeads

In this study, an engineered high-motility bacterium ΔppGpp *S. typhimurium* strain SHJ2037 was employed. Microbeads were attached to the surface of the bacteria to produce bacteriobots using streptavidin–biotin conjugation. The bacteriobots were observed using a confocal scanning microscope. The microbeads were coated with streptavidin-PerCP-Cy5.5 providing red fluorescence on the surface of microbeads, and the bacteria expressed engineered green fluorescence protein (EGFP) to display green fluorescence, as shown in Figure 1d. The bacterial membranes were coated with biotin prior to their attachment to the microbeads.

2.2.2. Motility Analysis of Dual-Tumor-Targeting Bacteriobots

The motility of the bacteriobots was observed on an agarose-coated petri dish under the field of microscope and then tracked and analyzed with a MATLAB program. As shown in Figure S5a,b, the bacteriobots had greater displacement owing to propulsion of the attached bacteria. However, the microbeads showed almost no displacement. Furthermore, the displacement of the bacteriobots during 1 min was almost 45 ± 15 µm, while the displacement of the microbeads was only 6 ± 3 µm due to the Brownian motion of the microbeads and bacterial collision in the solution (Figure S5c, Supporting Information). Therefore, the bacteriobots had excellent motility compared to the microbeads alone due to the conjugation with the mobile bacteria.

2.2.3. Cellular Uptake and Tumor Targeting Analysis of Dual-Tumor-Targeting Bacteriobots

To investigate the receptor-mediated cellular uptake of nanoparticles released from the HA microbeads, PLGA coumarin-6 nanoparticle-loaded HA microbeads were incubated with cancer cells (4T1) overexpressing the CD 44 receptor or CD 44 negative normal fibroblast NIH/3T3 cells. As seen in the confocal microscopy **Figure 2**, enhanced fluorescent signals were visualized in the cytoplasm of the HA microbead-treated 4T1 cells, demonstrating that the HA microbeads are readily taken up by the 4T1 cells (Figure 2b). In contrast, in 4T1 cells pretreated with a high dose of free HA to block the CD 44 receptors prior to HA-microbeads treatment, a reduction in intracellular fluorescence was observed Figure 2c, suggesting CD 44-specific cellular uptake of HA microbeads. In the NIH/3T3 cells without the CD 44 receptor, a very weak signal was detected (Figure 2e). Both 4T1 and NIH/3T3 cells treated with coumarin-6 nanoparticle-loaded HA microbeads were subject to flow cytometry (FACScan) analysis (Figure 2f–i), which showed enhanced fluorescence intensity in the CD 44-overexpressed 4T1 cells compared to that of the NIH/3T3 and CD 44-receptor-blocked 4T1 cells. Since the size of the micorbeads is 8 µm, the intracellular uptake of microbeads is not possible as microbeads are much bigger in size than that of cells. However, the presence of fluorescence could be explained by the cell surface tethering of HA microbeads by CD 44 receptors based interaction, which is over expressed in cancer cells,[12] followed by subsequent degradation of the HA microbeads causing release the nanoparticles. Since the release nanoparticles are in close proximity to the cells, the cells readily internalize them. However, NIH/3T3 cells, which lack CD 44 receptor, no surface tethering HA microbeads on to the cell surface could be possible and hence no cellular internalization of the nanoparticles by cells. A similar result is obtained upon blocking CD 44 receptors through the addition of excess of HA. These results suggested that the nanoparticle-loaded HA microbeads specifically bind to CD 44 and could release the nanoparticles, which could successfully internalized by the cells. These results suggested that the nanoparticle-loaded HA microbeads specifically bind to CD 44 and could release the nanoparticles.

In order to check the chemotaxis potential of bacteriobots, an agarose hydrogel-based microfluidic channel was prepared to investigate the ability of the bacteriobots to target 4T1 tumor cells. Chemotaxis motion of the bacteriobots was video recorded inside the experimental region of the channel and

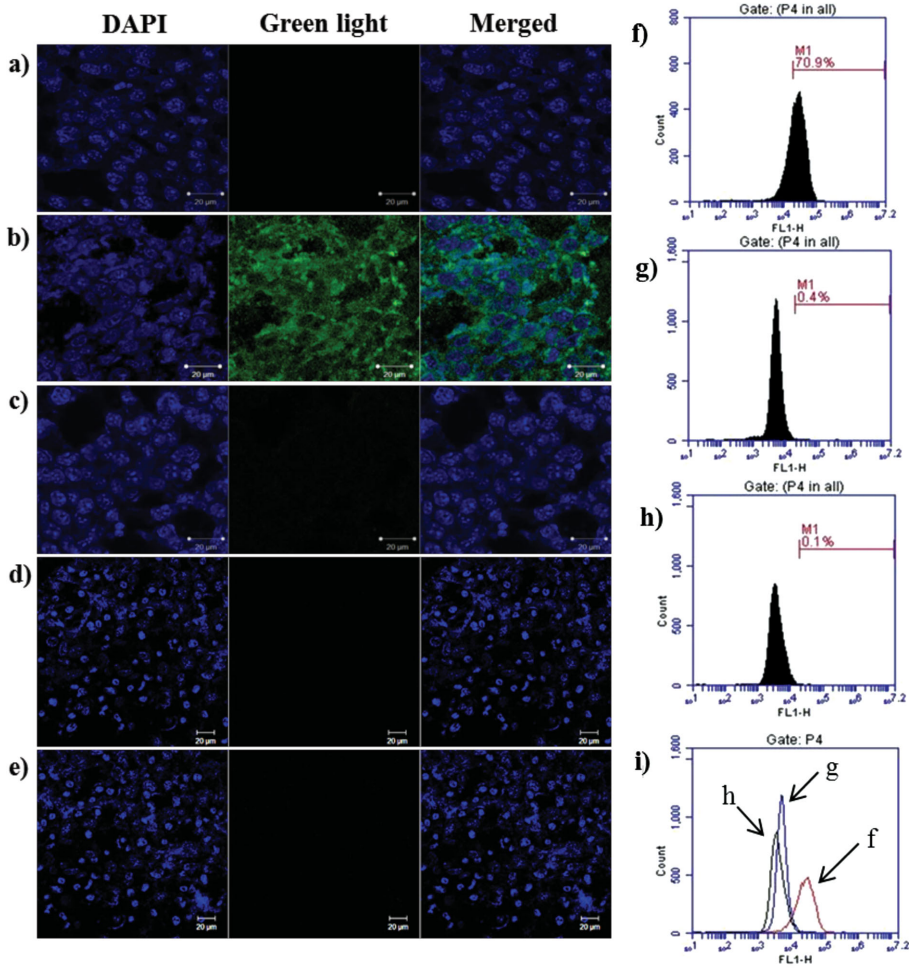

Figure 2. Confocal microscopy images and FACS analysis of the cellular uptake of PLGA coumarin nanoparticles from HA–Mal microbeads, a) Untreated 4T1 cells, b) 4T1 cells with HA-Mal microbeads loaded with PLGA coumarin nanoparticles, c) 4T1 cells with HA microbeads loaded with PLGA coumarin nanoparticles after HA treatment, d) Untreated NIH/3T3 cells, and e) NIH/3T3 cells with HA microbeads loaded with PLGA coumarin nanoparticles. Flow cytometry analysis of HA–malemide beads loaded with PLGA coumarin nanoparticles. f) 4T1 (CD 44 positive) cells, g) CD 44 blocked 4T1 cells, h) NIH/3T3 cells (CD44 negative) and i) all three FACS analyses combined.

analyzed using MATLAB. The tracked motion trails of the bacteriobots are shown in **Figure 3**a. The starting points of all the bacteriobots were grouped to the point (0, 0), which led to an end point distribution of the movement of the bacteriobots, as shown in Figure 3b. Also shown in Figure 3b, the majority of bacteriobots moved towards the chemoattractant 4T1 cell side, and the velocity in chemoattractant direction (horizontal direction) was 0.43 μm s^{-1}, whereas the velocity in the non-chemoattractant direction (vertical direction) was only 0.05 μm s^{-1}. The result demonstrated that bacteriobots sensitively reacted to chemoattractant secreted by tumor cells, which enabled the bacteriobots to target cancer cells specifically. In addition, owing to the random motion of bacteria, bacteriobots also drew displacements along non-chemoattractant direction (vertical direction). However, after the cancelation of positive and negative displacement, a little average velocity was merely evaluated as 0.05 μm s^{-1}. Theoretically, bacteriobots should not show any average displacement along vertical direction. However, in reality, there existed complicated factors that affect the motion of bacteriobots in microscale, such as, Brownian motion, collision of surrounding bacteria and other unknown factors. These complicated factors could not cancel to each other, which resulted in slight disequilibrium in the motion of bacteriobots. Additionally, as the non-chemoattractant directional velocity was almost 10 times smaller comparing with the chemoattractant directional velocity, we can conclude that the bacteriobots retained their bacterial chemotactic ability even after the assembly of the bacteria and microbeads. Therefore, bacteriobots can target tumor cells via molecular signals secreted by the tumor cells.

There has been no prior knowledge or report, which illustrates an experiment to determine the chemoattractant, tumor cell targeting, and tumor cell killing efficacy of these bacteriobots against cancer cells in cell culture condition all together, we have custom developed a new type of chamber on a petri dish with collagen-coated coverslips (Figure S7, Supporting Information). NIH/3T3 and 4T1 cells were seeded over the collagen-coated cover slips and placed in two different areas of

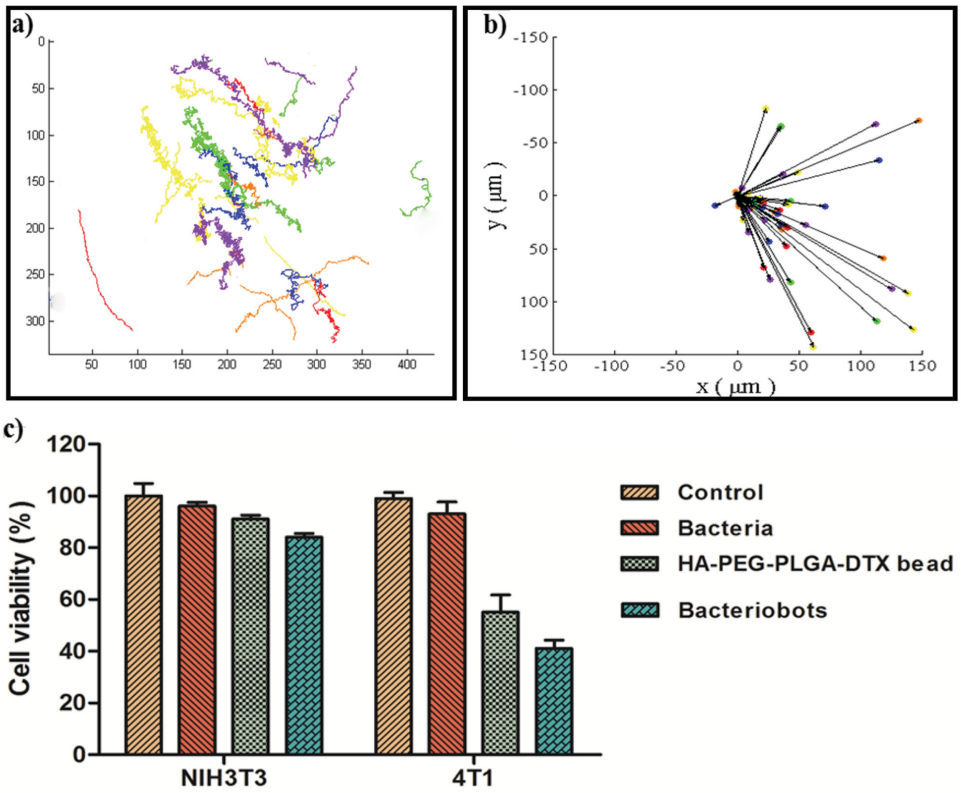

Figure 3. a) Movement tracking image of dual tumor-targeting bacteriobots. b) The distribution of the movement of the bacteriobots end points when the starting points are moved to the same time (0, 0). c) *In-vitro* antitumor activity comparison of bacteriobots, bacteria, drug-loaded HA microbeads, and control groups in NIH/3T3 and 4T1 cells in a chamber based on a petri dish and gelatin-coated coverslips.

the petriplate and a hole was made in the center of the cap of petri dish then 200 μm pipet-tip was inserted to the hole so that bacteria, PLGA–DTX nanoparticle-loaded HA microbeads, and the bacteriobots could be dropped smoothly and fairly. Before and after dropping, cells were incubated for 24 h. Since the bacteria were involved in this study all the cell lines were grown in antibiotics free media. In order to prevent the migration of cells from the cover slips to petri plate we have used sterile non-cell culture plates. The morphology of cells was observed using a microscope (Figure S8, Supporting Information), and cell viability was measured using the MTT assay. As shown in Figure 3c, the NIH/3T3 cells maintained high cellular viability (greater than 85%) across all the treatment conditions. The bacteria showed a slight cytotoxic effect to the 4T1 tumor cells, and the drug-encapsulated microbeads were highly cytotoxic because of the diffusion of the drug from the microbeads. Furthermore, the bacteriobots displayed enhanced therapeutic effect owing to the synergistic effect of the DTX and bacteria.

These results suggest that bacteriobots can enhance the therapeutic effect of cancer drugs compared to the pure drug-embedded particles through bacterial propulsion, and HA microbeads upon injection of the bacteriobots into the arterial circulation, would be carried by both the blood flow and through bacterial propulsion to the capillary bed, where they would be embolized and can also be taken up by tumor cells overexpressing CD 44 receptors. HA microbeads could also be degraded enzymatically by enzyme such as hyaluronidases, which are abundant in cytoplasmic compartments of the tumor cells thereby leading to facilitate intercellular delivery of drugs. Based on these results, bacteriobots can specifically accumulate to the site of tumor tissue by their dual-targeting ability and then migrate into the internal part of tumor tissue, while HA microbeads can attach to CD 44 receptors and be taken up by cells. Then, the drug loaded in the microbeads can be released to kill the tumor cells.

3. Conclusion

In order to fabricate bacteria-driven microbeads capable of delivering anticancer drug to the cancer cells, lots of challenges have to be addressed. First of all, a suitable bacterium has to be selected, which could selectively target the cancer cells. For this purpose our group has previously screened different mutants of *S. typhimurium* and identified strain of *S. typhimurium* with a defect in guanosine 5′-diphosphate-3′-diphosphate synthesis (ΔppGpp *S. typhimurium*) and carrying a cytotoxic agent such as cytolysinA (ClyA), a pore-forming bacterial toxin, which could effectively target tumor and regresses the tumors.[27] Since these bacteria have self-propelling abilities, which could be harnessed for driving the any therapeutic moiety attached on it. Second, tumor stroma-targeting microbeads have to be fabricated, which could selectively target and degrade in the tumor

environment. For this purpose, we have used HA a natural polymer, which could be easily degradable by the hyaluronidases (Hyals) enzyme whose levels are reported to be higher in various malignant tumors such as prostate, head, and neck, colorectal, brain, and metastatic breast cancer. Third, in order to propel the microbead successfully in one direction, the number of bacteria attached on to the cells has to be controlled. In this study, tumor-targeting attenuated *S. typhimurium* was attached to the surface of HA microbeads via streptavidin–biotin conjugation, thereby by controlling the streptavidin–biotin conjugation, we could easily control the number of bacteria attached on the surface of the microbeads so that the net self-propelling force of all bacteria enables the microbeads to move in a single direction.

In this study, dual-tumor-targeting therapeutic bacteriobots were developed with engineered *S. typhimurium* and drug nanoparticle-encapsulated HA microbeads. The drug-loaded microbeads showed a moderated drug release pattern and high cytotoxicity to tumor cells. Bacteriobots were prepared through biotin–streptavidin conjugation, leading to enhanced motility compared to its counterparts with no biotin–streptavidin conjugation. In addition, bacteriobots showed high chemotactic motion towards 4T1 cells, indicating their ability to specifically target tumor cells. Furthermore, through interaction with CD 44 receptors, HA tumor cells, demonstrating their ability to also specifically target tumor cells, efficiently took up microbeads. Based these dual tumor-targeting abilities, HA microbead-based bacteriobots are a promising potential tumor therapy. However the conversion of this technology to clinical applications there are still lots of challenges to be addressed such as: i) the number of bacteriobots to be used for the optimal delivery of drug to a target site; ii) the motility profile of these bacteriobots against the direction of blood flow; iii) immunological, in vivo and long-term toxicity effect upon interaction of bacteriobots with tissues.

4. Experimental Section

Synthesis of Maleimide-Functionalized Hyaluronic Acid (HA-Mal): The maleimide moiety was functionalized onto hyaluronic acid (HA) (M_W = 0.48 MDa) according to a previously reported method.[25] Briefly, at room temperature (RT), 100 mg of HA was dissolved in 50 mL of 0.1 M MES buffer. To the solution of HA, EDC (0.75 mmol, 144 mg) and NHS (0.75 mmol, 86 mg) were added to activate the carboxylic acid groups of HA. After 30 min of stirring, 0.25 mmol of AEM dissolved in 50 mL of 0.1 M MES buffer was added to the mixture and stirred for 4 h at RT. The resulting mixture was dialyzed against 50×10^{-3} M NaCl for one day and then with deionized water followed by lyophilization. The DS, defined as the number of maleimide groups per 100 disaccharide rings of the HA, was determined by ^{1}H NMR analysis.

Preparation of PLGA–DTX Nanoparticles: Nanoparticles were synthesized via the emulsion solvent evaporation technique[28] with slight modifications. Briefly, 100 mg of PLGA and 10 mg of docetaxel (DTX) were dissolved in 5 mL of dicholoromethane (DCM), which formed the organic phase. Under vigorous stirring, the organic phase was then slowly added to the aqueous phase containing 0.25% polyvinylalcohol (PVA), followed by sonication in an ice water bath for 5 min. The resulting emulsions were then stirred overnight resulting in the complete evaporation of the organic phase. The resulting solution was centrifuged at 15 000 rpm for 30 min. The pellet obtained was further suspended in deionized water (DW) and lyophilized. The lyophilized product was used for all further studies and analyses. The encapsulation efficiency of the DTX was determined as explained in Section 3.1. (Supporting Information).

Preparation of PLGA–DTX Nanoparticle-Encapsulated HA Microbeads: A microfluidic channel containing a cross-junction was prepared using the conventional photo and soft-lithography method.[29] For the CP solution, a co-solvent mixture (v/v 10/1) of hexadecane (Sigma–Aldrich Chemical Co.) and sorbitan monolete (Span 80, Sigma–Aldrich Chemical Co.) was used. The DP solution contained 1×10^{-3} M four-arm-thiolated polyethylene glycol (PEG–SH) (SUNBIO). PEG–SH droplets that formed at the cross-junction were then cross-linked outside of the microfluidic channel using 1×10^{-3} M HA-Mal. After the preparation of the microbeads, the buffer was changed to DW. To prepare the microbeads compartmentalized with PLGA–DTX nanoparticles, the DP solution was made by mixing 1% (w/v) PLGA–DTX nanoparticles in a vortex mixer for 30 s and loaded on to the microfluidic channel.

Preparation of Dual-Tumor-Targeting Bacteriobots by Immobilizing S. Typhimurium on PLGA–DTX Nanoparticle-Encapsulated HA Microbeads: To prepare the bacteriobots, biotin–streptavidin conjugation was employed to attach the bacteria to the microbeads.[16] Briefly, HA microbeads (1×10^6 mL^{-1}) were coated with 500 µg of streptavidin-labeled by Cy5.5 (PerCP-Cy5.5) (BD Biosciences, San Diego, CA) for 1 h and then centrifuged at 8000 rpm for 5 min. S. typhimurium (1 mL, OD_{600} value = 0.8) were modified with 500 µg EZ-Link NHS-LC-Biotin (Thermos Scientific, Rockford, IL) for 1 h. Then, the bacteriobots were prepared by mixing the bacteria and microbeads at 37 °C in an incubator for 30 min. Finally, the bacteriobots were observed with a confocal laser scanning microscope (LSM510, Zeiss, Germany).

Cell Viability Assay of Dual-Tumor-Targeting Bacteriobots: The in vitro cell viability of the HA-Mal microbeads and PLGA–DTX nanoparticle-loaded microbeads were analyzed using an MTT assay. Briefly 5×10^3 cells per well were seeded in a 96-well plate and incubated at 37 °C for 12 h. After incubation, the medium was drained off, and the cells were washed with PBS. After washing, 100 µL of Opti-MEM media was added to the samples. After 6 h incubation, the Opti-MEM media were drained off, 100 µL of fresh DMEM media was added, and the cells were incubated for 24 h at 37 °C. The viability of the cells was then assayed using the MTT assay (Promega, USA). To test the cell viability of the bacteria-driven microbeads, the cells (4T1 and NIH/3T3) were first grown on a collagen-coated cover glass and placed in a petri dish containing DMEM media. To drop the bacteria-driven microbeads smoothly onto the petri dish, a hole was made in the center of the cap of the petri dish, and then a 200-µm-pipet tip was placed into the hole. After dropping in the bacteria-driven microbeads, the cells were incubated for 24 h.

Cellular Imaging of Dual-Tumor-Targeting Bacteriobots: 4T1 and NIH/3T3 cells were cultured in RMPI 1640 and DMEM medium comprising 10% v/v FBS and 1% v/v antibiotic–antimitotic solution (Gibco-BRL/Invitrogen). The incubating conditions were 37 °C in a 5% CO_2 atmosphere. To determine the cellular uptake of the nanoparticle-loaded HA microbeads, both 4T1 and NIH3T3 cells (10^5 cells per well) were seeded in Lab-Tek chamber slides. After 24 h, PLGA coumarin-6 nanoparticle-loaded HA microbeads were added to both the 4T1 and NIH/3T3 cells and incubated in the dark for 4 h at 37 °C. After incubation, the media were aspirated, and the cells were washed three times with PBS followed by treatment with 4% paraformaldehyde. Following removal of the PBS, the nucleus was stained with Gold antifade reagent with 4′,6-diamidino-2-phenylindole (DAPI) for 20 min at 37 °C. The fluorescence was then visualized using a confocal laser scanning microscope. For the competitive inhibition study, 8 mg mL^{-1} of HA polymer was added to the sample 4 h prior to block the CD 44 receptor, followed by subsequent washing with PBS five times.

For the flow cytometry analysis, PLGA coumarin-6 nanoparticle-loaded HA microbeads were added to both 4T1 and NIH/3T3 cells (1×10^6 cells per well) and incubated for 4 h. After incubation, the medium was removed, and the cells were washed with PBS three times. After the PBS wash, the cells were harvested and analyzed using a FACScan flow cytometer.

Supporting Information

Supporting Information is available from the Wiley Online Library or from the author.

Acknowledgements

S.U. and S.Z. contributed equally to this work. Sukho Park and In-Kyu Park are co-corresponding authors. This research was supported by the Pioneer Research Center Program (2009-0082954 and 2014M3C1A3053035) through the National Research Foundation of Korea funded by the Ministry of Science, ICT & Future Planning.

Received: July 15, 2015
Revised: September 10, 2015
Published online: November 19, 2015

[1] R. L. Siegel, K. D. Miller, A. Jemal, *CA: A Cancer J. Clin.* **2015**, *65*, 5.
[2] R. K. Jain, T. Stylianopoulos, *Nat. Rev. Clin. Oncol.* **2010**, *7*, 653.
[3] O. Trédan, C. M. Galmarini, K. Patel, I. F. Tannock, *J. Natl. Cancer Inst.* **2007**, *99*, 1441.
[4] S. Uthaman, S. Maya, R. Jayakumar, C. S. Cho, I. K. Park, *J. Nanosci. Nanotechnol.* **2014**, *14*, 694.
[5] E. N. Harris, J. A. Weigel, P. H. Weigel, *J. Biol. Chem.* **2008**, *283*, 17341.
[6] R. Prevo, S. Banerji, D. J. P. Ferguson, S. Clasper, D. G. Jackson, *J. Biol. Chem.* **2001**, *276*, 19420.
[7] A. Aruffo, I. Stamenkovic, M. Melnick, C. B. Underhill, B. Seed, *Cell* **1990**, *61*, 1303.
[8] J. Entwistle, C. L. Hall, E. A. Turley, *J. Cell Biochem.* **1996**, *61*, 569.
[9] Y. Takei, A. Maruyama, A. Ferdous, Y. Nishimura, S. Kawano, K. Ikejima, S. Okumura, S. Asayama, M. Nogawa, M. Hashimoto, Y. Makino, M. Kinoshita, S. Watanabe, T. Akaike, J. J. Lemasters, N. Sato, *FASEB J.* **2004**, *18*, 699.
[10] K. S. Kim, W. Hur, S. J. Park, S. W. Hong, J. E. Choi, E. J. Goh, S. K. Yoon, S. K. Hahn, *ACS Nano* **2010**, *4*, 3005.
[11] a) H. Yin, F. Zhao, D. H. Zhang, J. Li, *Int. J. Pharm.* **2015**, *483*, 169; b) X. Y. Cao, L. Tao, S. H. Wen, W. X. Hou, X. Y. Shi, *Carbohydr. Res.* **2015**, *405*, 70.
[12] V. J. Wielenga, K.-H. Heider, G. Johan, A. Offerhaus, G. R. Adolf, F. M. van den Berg, H. Ponta, P. Herrlich, S. T. Pals, *Cancer Res.* **1993**, *53*, 4754.
[13] H. Y. Yoon, H. Koo, K. Y. Choi, S. J. Lee, K. Kim, I. C. Kwon, J. F. Leary, K. Park, S. H. Yuk, J. H. Park, *Biomaterials* **2012**, *33*, 3980.
[14] M. S. Rajput, P. Agrawal, *Indian J. Cancer* **2010**, *47*, 458.
[15] M. C. Burgmans, Y. H. Kao, F. G. Irani, E. L. Dames, T. K. B. Teo, A. S. W. Goh, P. K. H. Chow, K. H. Tay, R. H. G. Lo, *J. Vasc. Interv. Radiol.* **2012**, *23*, 1294.
[16] S. J. Park, S. H. Park, S. Cho, D. M. Kim, Y. Lee, S. Y. Ko, Y. Hong, H. E. Choy, J. J. Min, J. O. Park, S. Park, *Sci. Rep.-UK* **2013**, 3.
[17] U. N. Le, H. S. Kim, J. S. Kwon, M. Y. Kim, V. H. Nguyen, S. N. Jiang, B. I. Lee, Y. Hong, M. G. Shin, J. H. Rhee, H. S. Bom, Y. Ahn, S. S. Gambhir, H. E. Choy, J. J. Min, *Mol. Ther.* **2011**, *19*, 951.
[18] S. Cho, S. J. Park, S. Y. Ko, J. O. Park, S. Park, *Biomed. Microdevices* **2012**, *14*, 1019.
[19] S. J. Park, Y. K. Lee, S. Cho, S. Uthaman, I. K. Park, J. J. Min, S. Y. Ko, J. O. Park, S. Park, *Biotechnol. Bioeng.* **2015**, *112*, 769.
[20] M. Kojima, Z. H. Zhang, M. Nakajima, T. Fukuda, *Biomed. Microdevices* **2012**, *14*, 1027.
[21] R. Mhanna, F. M. Qiu, L. Zhang, Y. Ding, K. Sugihara, M. Zenobi-Wong, B. J. Nelson, *Small* **2014**, *10*, 1953.
[22] V. Magdanz, S. Sanchez, O. G. Schmidt, *Adv. Mater.* **2013**, *25*, 6581.
[23] P. L. Venugopalan, R. Sai, Y. Chandorkar, B. Basu, S. Shivashankar, A. Ghosh, *Nano Lett.* **2014**, *14*, 1968.
[24] P. Burgos, M. Geoghegan, G. J. Leggett, *Nano Lett.* **2007**, *7*, 3747.
[25] R. Jin, P. J. Dijkstra, J. Feijen, *J. Controlled Release* **2010**, *148*, e41.
[26] A. Anitha, S. Uthaman, S. V. Nair, R. Jayakumar, V. K. Lakshmanan, *J. Biomed. Nanotechnol.* **2013**, *9*, 335.
[27] V. H. Nguyen, H. S. Kim, J. M. Ha, Y. J. Hong, H. E. Choy, J. J. Min, *Cancer Res.* **2010**, *70*, 18.
[28] Z. Xu, W. Gu, J. Huang, H. Sui, Z. Zhou, Y. Yang, Z. Yan, Y. Li, *Int. J. Pharm.* **2005**, *288*, 361.
[29] Y. Xia, G. M. Whitesides, *Annu. Rev. Mater. Sci.* **1998**, *28*, 153.